SLAC – PUB – 4660
June 1988
(A)

A Final Focus System for Flat-Beam Linear Colliders*

KATSUNOBU OIDE

Stanford Linear Accelerator Center
Stanford University, Stanford, California 94309

ABSTRACT

A final focus system is designed for a flat-beam linear collider with the parameters suggested by R. B. Palmer. A method of chromaticity correction which uses one family of sextupole is realized so as to correct both horizontal and vertical chromaticities simultaneously. A computer code has been written to find the solution, and a result with a momentum acceptance twice that of Palmer's requirement is obtained. It is shown that the designed optics is almost at the limit of focusing which is given by the synchrotron radiation in the final quadrupole.

⋆ Work supported by the Department of Energy, contract DE–AC03–76SF00515

1. Introduction

Among numbers of designs of future linear colliders, the flat-beam collider proposed by R. B. Palmer[1] seems to have a great feasibility with conventional technologies. He has shown that the flat beam scheme has a lot of advantages in various parts of the collider including the final focus system. In this paper I will present a design of a final focus optics which satisfies the following Palmer's requirements:

Center-of-mass energy	E_{CM}	$= 1$ TeV,		
Beta function at collision point	β_x^*	$= 14$ mm,	β_y^*	$= 43\ \mu$m,
Normalized emittance	$\varepsilon_{\mathrm{Nx}}$	$= 2.5 \times 10^{-6}$ m,	$\varepsilon_{\mathrm{Ny}}$	$= 2.5 \times 10^{-8}$ m,
Momentum acceptance	$\lvert\Delta p/p\rvert$	≤ 0.15 %,		

under the following restrictions:

Pole-tip field of the final quadrupole	$B_0 \leq 1.4$ T,
Length from the face of the final quad to the collision point	$\ell^* = 0.4$ m,
Quadrupole half aperture	a $\geq 100\ \mu$m.

These values correspond to the 17 mm wavelength case of Ref. 1. It is expected to be possible to achieve these values using a scaling law from the SLC design[2] or the one-dimensional system,[3] but this still needs verification by a detailed optics design. In particular, the synchrotron radiation from quadrupoles and bends requires a study with specific optics parameters, this yields a serious limit on focusing as we will see in Section 4.

2. Chromaticity-correction scheme

The optics designed here uses a chromaticity-correction scheme with sextupoles and bends. For the flat beam linear collider, where the ratio β_x^*/β_y^* is larger than 300, the vertical chromaticity is much larger than the horizontal one, so it is natural to use one family of sextupoles which mainly contributes to correct the vertical chromaticity. Decreasing the number of sextupoles in the system has the merit of making the total length of the system shorter and the residual geometric nonlinear aberration smaller. However, in the actual optics the horizontal chromaticity still needs a weak correction, and there is a special configuration of optics to correct both x and y chromaticities simultaneously by one family of sextupole as described below.

Now let us consider a simplified model of a final focus system as shown in Fig. 1.

Here we take account of the chromatic effect only from the final quadrupole and the sextupole, and ignore the chromaticity from the other parts of the system. Actually we have two sextupoles in the system, but their chromatic effects are equivalent owing to the $-I$ transformation between them, and it enables us to represent them by one sextupole in this model. We choose the Twiss parameters at the entrance sextupole as $\alpha = \alpha_S = 0$ and $\beta = \beta_S$, and at the exit collision point as $\alpha^* = 0$ and $\beta = \beta^*$. The transfer matrix from the entrance to the exit is written for the design particle as

$$M_0 = \begin{pmatrix} \sqrt{\frac{\beta_0^*}{\beta_S}} \cos\mu & \sqrt{\beta_0^* \beta_S} \sin\mu \\ -\frac{1}{\sqrt{\beta_0^* \beta_S}} \sin\mu & \sqrt{\frac{\beta_S}{\beta_0^*}} \cos\mu \end{pmatrix} , \tag{2.1}$$

where μ is the phase advance between the sextupole and the collision point. We introduce a parameter χ to represent momentum deviation as

$$\chi \equiv \frac{\Delta p/p}{1 + \Delta p/p} , \tag{2.2}$$

which enables us to write the focusing strength of the final quad and the focusing component of the sextupole as

$$k = (1-\chi)k_0 \qquad \text{and} \qquad k_S = \chi k'\eta \quad , \tag{2.3}$$

where k_0 is the strength of the quadrupole for the design momentum, and k' and η are the strength of the sextupole and the horizontal dispersion at the sextupole, respectively. Thus we obtain the transfer matrix for off-momentum particles in terms of χ:

$$\begin{aligned} M &= \begin{pmatrix} 1 & \ell \\ 0 & 1 \end{pmatrix} \begin{pmatrix} 1 & 0 \\ -k & 1 \end{pmatrix} \left[\begin{pmatrix} 1 & \ell \\ 0 & 1 \end{pmatrix} \begin{pmatrix} 1 & 0 \\ -k_0 & 1 \end{pmatrix} \right]^{-1} M_0 \begin{pmatrix} 1 & 0 \\ -k_S & 1 \end{pmatrix} \\ &= \begin{pmatrix} 1+\chi k_0\ell & -\chi k_0\ell^2 \\ \chi k_0 & 1-\chi k_0\ell \end{pmatrix} M_0 \begin{pmatrix} 1 & 0 \\ -\chi k'\eta & 1 \end{pmatrix} \quad . \end{aligned} \tag{2.4}$$

We can now calculate the off-momentum beta function at the collision point using (2.1) and (2.4):

$$\begin{aligned} \beta^* &= M_{11}^2\beta_S + M_{12}^2/\beta_S \\ &= \beta_0^* \left\{ \left[(1+\chi k_0\ell)\cos\mu + \chi\xi\sin\mu - \chi k'\beta_S\eta\left((1+\chi k_0\ell)\sin\mu - \chi\xi\cos\mu\right)\right]^2 \right. \\ &\qquad \left. + \left[(1+\chi k_0\ell)\sin\mu - \chi\xi\cos\mu\right]^2 \right\} \quad , \end{aligned} \tag{2.5}$$

where we have defined the parameter

$$\xi \equiv k_0\ell^2/\beta_0^* \quad , \tag{2.6}$$

which represents the amount of the chromaticity of the system. It is about 1.5×10^4 for vertical and 300 for horizontal in our design. The first order of χ in (2.5) is

$$\beta^* = \beta_0^* \left(1 + 2\chi k_0\ell - \chi k'\beta_S\eta\sin 2\mu\right) \quad , \tag{2.7}$$

where the second term is always small because $k_0\ell$ is order of unity. In the third term the magnitude of $k'\beta_S\eta$ will be set equal to ξ as shown later, therefore it is much larger than unity, so that $\sin 2\mu$ must be close to zero to cancel the linear dependence of β^* on χ. This is satisfied by choosing the phase advance μ as near $(N + \frac{1}{2})\pi$ or $N\pi$, where N is an integer. We call them as Mode I and Mode II, respectively, and will see these two modes have different effects on the chromaticity correction.

The Mode I ($\mu \approx (N + \frac{1}{2})\pi$) correction is achieved by setting

$$k_0 \ell \sin\mu - \xi \cos\mu = 0 \quad , \tag{2.8}$$

which makes the momentum dependence of M_{12} zero. By substituting (2.8) into (2.5), we find that all the chromatic effects of β^* disappear when we set the strength of the sextupole to be

$$k' \beta_S \eta = \mathrm{sgn}(\xi)\sqrt{\xi^2 + k_0^2 \ell^2} \approx \xi \quad . \tag{2.9}$$

On the other hand, the Mode II ($\mu \approx N\pi$) correction is done by

$$\sin\mu = 0 \quad . \tag{2.10}$$

We substitute (2.10) into (2.5) and using $\xi \gg k_0 \ell$, then obtain

$$\beta^* = \beta_0^*(1 + \chi^2 \xi(2k'\beta_S\eta + \xi) + \chi^4 \xi^2 (k'\beta_S \eta)^2) \quad . \tag{2.11}$$

In the Mode II the chromatic effect on beta function is not completely cancelled, but there appears a momentum region where β^* is smaller than the nominal value β_0^* as shown in Fig. 2. This region is expressed as

$$\chi^2 \leq -\frac{2k'\beta_S\eta + \xi}{\xi(k'\beta_S\eta)^2} \ , \tag{2.12}$$

and the size of this region becomes its maximum when we choose the sextupole strength as

$$k'\beta_S\eta = -\xi \quad , \tag{2.13}$$

which has the same amplitude but opposite sign as the Mode I correction. Thus the maximum momentum acceptance of Mode II is given by

$$|\chi| \leq \frac{1}{\xi} \quad . \tag{2.14}$$

The fact that these two correction modes have the opposite sign to each other makes the one-family-sextupole chromaticity correction possible for both x and y planes simultaneously. Because the momentum acceptance is given by the Mode II as Eq. (2.14), and ξ_y is much larger than ξ_x in the flat-beam collider, we should apply Mode II to the horizontal correction and Mode I to the vertical to get a large momentum acceptance. The conditions (2.9) and (2.13) are simultaneously satisfied by setting the ratio of the beta functions at the sextupole as

$$\frac{\beta_{Sy}}{\beta_{Sx}} = \frac{\xi_y}{\xi_x} \quad , \tag{2.15}$$

which is about 50 in our design. Since the momentum acceptance of the system is determined only by the horizontal chromaticity, a large horizontal/vertical ratio of β^*'s makes the chromaticity correction easier.

3. Finding the solution

The actual method of finding the solution I used here did not explicitly contain the conditions of the single-family-sextupole correction described in the previous section. The reason being that we should include higher order chromatic effects that were ignored in the simplified model, from the doublet configuration of the final quadrupoles, the thickness of the lenses, the other parts in the system, and so on. Instead of making an analytic formula with these effects, I took a practical way to find the solution, but the obtained result clearly showed the characteristics of the single-family-sextupole correction scheme. This method consisted of two steps. In the first step, I picked five points $\frac{\Delta p_j}{p}(j = -2..2)$ in the desired momentum acceptance δ with an equal separation, namely,

$$\frac{\Delta p_j}{p} = \frac{j}{2}\delta, \qquad j = -2..2 \ . \tag{3.1}$$

For each $\Delta p_j/p$ I calculated the linear optics independently and I ignored the geometric nonlinearity from the sextupoles in this step. Then I searched an optics which would satisfy the following conditions simultaneously:

$$\begin{aligned} &\beta_x^*(\frac{\Delta p_j}{p}) \le \beta_{0x}^*, \qquad \alpha_x^*(\frac{\Delta p}{p} = 0) = 0 \ , \\ &\beta_y^*(\frac{\Delta p_j}{p}) \le \beta_{0y}^*, \qquad \alpha_y^*(\frac{\Delta p}{p} = 0) = 0 \ , \end{aligned} \tag{3.2}$$

where j runs from -2 to 2. I made a computer code, named SAD/FFS,[4] which applied a multi-dimension Newton's method on finding the solution. Figure 3 shows the final focus optics obtained by this method. I took the strength of quadrupoles QA1-3 and QC1-5, the length of the straight sections LA1-3 and LC1-5, and the strength of the sextupole SD1 as the variables. During the solution search the optics between two sextupoles was kept as a $-I$ transformation to cancel the geometric nonlinearity. The bending angle, the total length of the system, and the mirror symmetry of the sextupole section were also preserved. The number of variables was chosen to be larger than the number of the imposed conditions. We chose the beta functions for the incoming beam to be $\beta_x = 11.6$ m and $\beta_y = 5.8$ m, those are near the values in the linac of Palmer's design. Thus the demagnification ratio became 1/29 for horizontal and 1/370 for vertical.

After a solution was found in the first step, I tested it in the second step by a particle-tracking simulation which took account of the nonlinearity of the sextupoles and the synchrotron radiation in the quadrupoles and bends. When this check failed, I changed the configurations bending angle etc., then backed up to the first step. After iterations a few I reached to the result of Fig. 3. The optics parameters are listed in Table 1.

Although this method has not explicitly used the conditions obtained in the previous section, the result has clear evidences of the single-family-sextupole correction. For an example the chromaticities are $\xi_x = 328$ and $\xi_y = 14,800$, those are nearly equal to the focusing components of the sextupole $k'\beta_x\eta = 347$ and $k'\beta_y\eta = 15,400$, respectively. Here we have calculated the values of ξ's using $\xi = \int K\beta ds$, where K is defined as $K \equiv k/\ell_Q$ with the length of quadrupole ℓ_Q, which is a generalization of (2.6) for thick lenses. The phase advances are resulted as $\mu_x \approx 2\pi$ and $\mu_y \approx \frac{3}{2}\pi$, which correspond to the Mode II and the Mode I correction, respectively.

Figure 4 shows the momentum dependence of the obtained beta functions at the collision point. The horizontal beta behaves as a quartic function due to the Mode II correction described by (2.11). We also see the vertical beta has only higher order components than quartic owing to the Mode I correction, which cancels all the terms less than quartic as we have seen in Section 2. The achieved momentum acceptance is $\Delta p/p \leq 0.3\%$, which is twice better than Palmer's requirement and agrees with the expectation by Eq. (2.14) if we substitute the value of the horizontal chromaticity $\xi = \xi_x = 328$.

4. Synchrotron radiation limit of focusing

Synchrotron radiation, especially in the final quadrupole, seriously limits the focusing of the beam. The incoherent energy spread generated by the synchrotron radiation in the final quadrupole changes the final spot size due to the chromatic effect of the final quadrupole itself. The vertical beam size of the flat-beam collider is almost at this limit. The minimum possible beam size is determined almost only by the normalized emittance ε_{Ny} as[5]

$$\sigma^*_{y\ \mathrm{min.}} = \left(\frac{7}{5}\right)^{\frac{1}{2}} \left[\frac{275}{3\sqrt{6\pi}} r_e \lambda\!\!\!^{-}_e F(\sqrt{K}\ell_Q, \sqrt{K}\ell^*)\right]^{\frac{1}{7}} (\varepsilon_{Ny})^{\frac{5}{7}} \ , \qquad (4.1)$$

where r_e and $\lambda\!\!\!^{-}_e$ is the classical electron radius and Compton wavelength, respectively. Equation (4.1) contains a dimensionless function F, which is a function of the length ℓ_Q and the strength $K \equiv k/\ell_Q$ of the quadrupole and ℓ^*. This has the form as shown in Ref. 5:

$$F(\sqrt{K}\ell_Q, \sqrt{K}\ell^*) = \int_0^{\sqrt{K}\ell_Q} \left(\sin\phi + \sqrt{K}\ell^* \cos\phi\right)^3 \left[\int_0^{\phi} \left(\sin\phi' + \sqrt{K}\ell^* \cos\phi'\right)^2 d\phi'\right]^2 d\phi \ . \qquad (4.2)$$

These values for our system give $F = 7.2$, and the minimum beam size calculated by Eq. (4.1) is 1.3 nm, which is about 30 % larger than Palmer's requirement. The dependence of the minimum beam size on F is 1/7th power, so that one cannot expect a big improve by changing the configuration of the final quadrupole.

We have a little more complication in the actual system. The minimum beam size (4.1) does not include the radiation caused by the horizontal focusing, which especially in the second final quadrupole makes an energy spread comparable with the final quadrupole. Besides, the vertical distribution of the beam becomes non-Gaussian, because the expected number of photons emitted per electron in the final quadrupole is very small; $\mathcal{N} = 0.35$ for our design. Instead of making a precise expression which includes these effects, I present here a numerical result in Fig. 5 obtained by the multi-particle tracking simulation.

In this simulation a random number series which has the spectrum of the synchrotron radiation[6] is used, and the effective vertical beam size is calculated from the luminosity of the simulated beam collision in the (x,y) plane at the collision point. This result has the same characteristics as the estimate we have seen in this section. The effective beam size does not depends on ℓ^*, when we changed the thickness of the final two quadrupoles proportionally to ℓ^* and the strength k of the final quadrupole becomes proportional to the inverse of ℓ^*. This is a consequence from (4.1), which does not depend on the longitudinal scale of the system. The minimum effective vertical beam size for our parameters is about 1.1 nm, which is not far from the value given by Eq. (4.1). We see the effective vertical beam size of Palmer's requirement is almost same as the limit of the focusing.

In the sextupole-bending chromaticity-correction scheme, the synchrotron radiation in the bending magnets also limits the focusing. The energy spread made in the bends between the sextupole and the final quadrupole affects to the vertical focusing in the same way as the radiation in the quadrupoles. This effect depends on the bending angle; if we increase it, the energy spread makes the final beam size larger, on the contrary if we decrease the bending angle, the sextupoles become stronger and the residual geometric nonlinearity also causes the final spot size to increase.

Figure 6 shows the dependence of the beam size on the total bending angle of the system, where the product of the bending angle and the strength of the sextupole is kept constant. There we find an optimum point for the bending angle near 1 mrad, which we adopted in this design.

Figure 6 also shows the increase of the horizontal beam size, which is caused by the horizontal emittance growth in the bends as discussed in Ref. 3. It is not so difficult to choose the bending angle small enough to make the emittance growth negligible, especially for the flat-beam linear collider whose horizontal emittance is not so small. We see in Fig. 6 the limit is about 4 mrad for our design.

5. Conclusion

We have studied a design of a final focus system for flat-beam colliders. We have seen that the chromaticity correction is possible using a single-family-sextupole correction scheme. This design has reached a “final” focusing limit due to the quantized synchrotron radiation in the final quadrupole. Further studies of this approach to a final focus design are required with emphasis on the required tolerance on various machine errors.

REFERENCES

1. R. B. Palmer, SLAC-PUB-4295 (1987).
2. K. L. Brown and J. E. Spencer, SLAC-PUB-2678 (1981).
3. A. Chao et al., CERN LEP-TH/87-48 (1987).
4. K. Hirata, Proceedings of the Second ICFA Beam Dynamics Workshop, Lugano (1988).
5. K. Oide, to be published.
6. K. Yokoya, KEK Report 85-9 (1985).

TABLE CAPTIONS

1. The list of parameters of the final focus system. This is written in SAD format: The keywords DRIFT, BEND, QUAD, and SEXT specify the type of the element. The keyword 'L=' is followed by the length of the element in meters. 'ANGLE=' specifies the bending angle in radians. 'K1=' and 'K2=' are the strength of quadrupoles and sextupoles, namely $\frac{B'\ell_Q}{B\rho}$ and $\frac{B''\ell_S}{B\rho}$, respectively. Positive signs mean horizontal focusing. The alignment of these elements are specified by the 'LINE' command. The beam parameters at the entrance is written in the 'ENTRANCE' element.

```
DRIFT LA1      =(L=  6.9376806)
      LA2      =(L= 42.3379557)
      LA3      =(L=  0.6672333)
      LS2      =(L=  0.1000000)
      LN2      =(L= 18.2306990)
      LN1      =(L=  3.0470206)
      LB0      =(L=  0.1000000)
      LX6      =(L=  0.1000000)
      LC5      =(L= 10.1555125)
      LC4      =(L= 68.1836864)
      LC3      =(L= 13.2796225)
      LX2      =(L=  0.0400000)
      LX1      =(L=  0.4000000);
BEND  B01      =(L= 30.0000000 ANGLE=  0.0003300)
      B02      =(L= 30.0000000 ANGLE=  0.0002600);
QUAD  QA1      =(L=  2.0000000 K1=     0.0362053)
      QA2      =(L=  2.0000000 K1=    -0.0642490)
      QA3      =(L=  2.0000000 K1=     0.0519296)
      QN3      =(L=  2.0000000 K1=    -0.0787193)
      QN2      =(L=  2.0000000 K1=     0.0911798)
      QN1      =(L=  1.0000000 K1=    -0.0199090)
      QC5      =(L=  2.0000000 K1=    -0.0608614)
      QC4      =(L=  2.0000000 K1=     0.0741367)
      QC3      =(L=  2.0000000 K1=    -0.0249200)
      QC2      =(L=  0.4000000 K1=     1.9285500)
      QC1      =(L=  0.4000000 K1=    -3.4161196);
SEXT  SD1      =(L=  2.0000000 K2=   -70.0000000);
MARK  ENTRANCE=(ALPHAX=0 BETAX=11.6 ALPHAY=0 BETAY=5.8
                 EMIX=2.5D-12 EMIY=2.5D-14 DP=0.003);
LINE  FFS      =(ENTRANCE
                 B02  LA1  QA1  LA2  QA2  LA3  QA3
                 LS2  SD1  SD1  SD1  SD1  LN2  QN3
                 LN1  QN2  LB0  B01  LB0  QN1  QN1
                 LB0  B01  LB0  QN2  LN1  QN3  LN2
                 SD1  SD1  SD1  SD1  LS2  QA3  LA3
                 QA2  LA2  QA1  LA1  B02  LX6  QC5
                 LC5  QC4  LC4  QC3  LC3  QC2  LX2
                 QC1  LX1   );
```

Table 1

FIGURE CAPTIONS

1. A simplified model for the final focus system. The final quadrupole of strength k is located at a distance ℓ from the collision point and a sextupole of strength k' is placed at the entrance of the system. M_0 is the transfer matrix from the sextupole to the collision point for the nominal momentum particle.

2. The beta function behaves as a quartic function when the Mode II correction is applied.

3. The final focus optics obtained by SAD/FFS. The upper figure shows the whole system of length 400 m and the lower around the collision point. The first character of each element specifies the type of the element as L:drift, B:bend, Q:quadrupole, and S:sextupole. The sextupole section has a mirror symmetry and the transformation between two sextupoles is $-I$ for both x and y planes.

4. Momentum dependence of the beta functions at the collision point. These exhibit the characteristics of the single-family-sextupole correction.

5. The effective vertical beam size as a function of the nominal beta β^*_{y0}. This result is obtained from multi-particle tracking with 2,000 particles. Three cases of ℓ^* are plotted, and there are no significant differences among them. The thickness of the final two quadrupoles are changed proportionally to ℓ^*. The solid line shows the case without the synchrotron radiation in the final two quadrupoles.

6. Vertical and horizontal beam sizes depend on the total bending angle of the system. These are also obtained from the tracking simulation. The product of the bending angle and the strength of the sextupole k' is kept constant. Two cases with and without the radiation in the bends are shown.

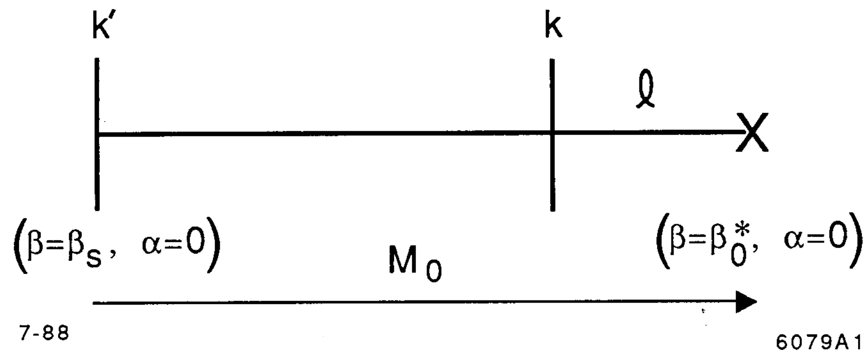

Fig. 1

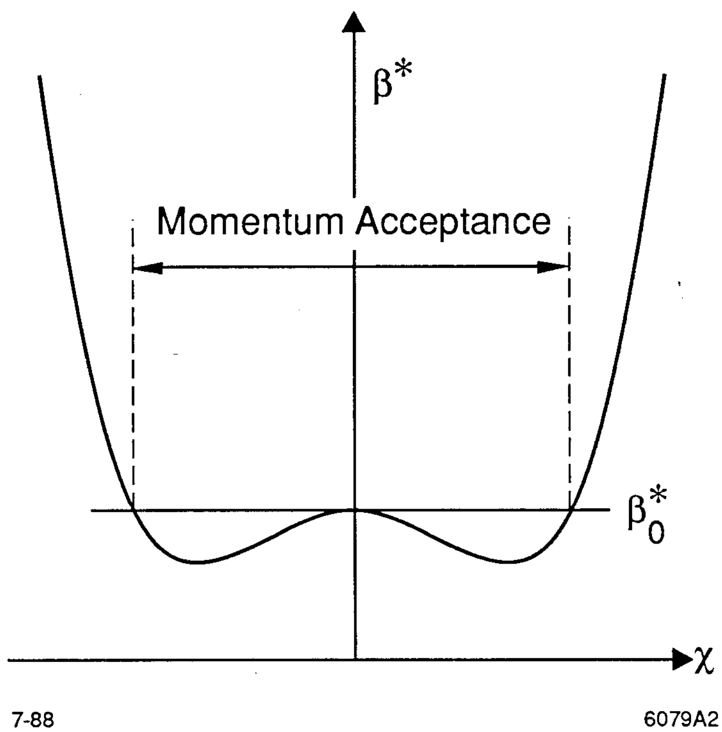

Fig. 2

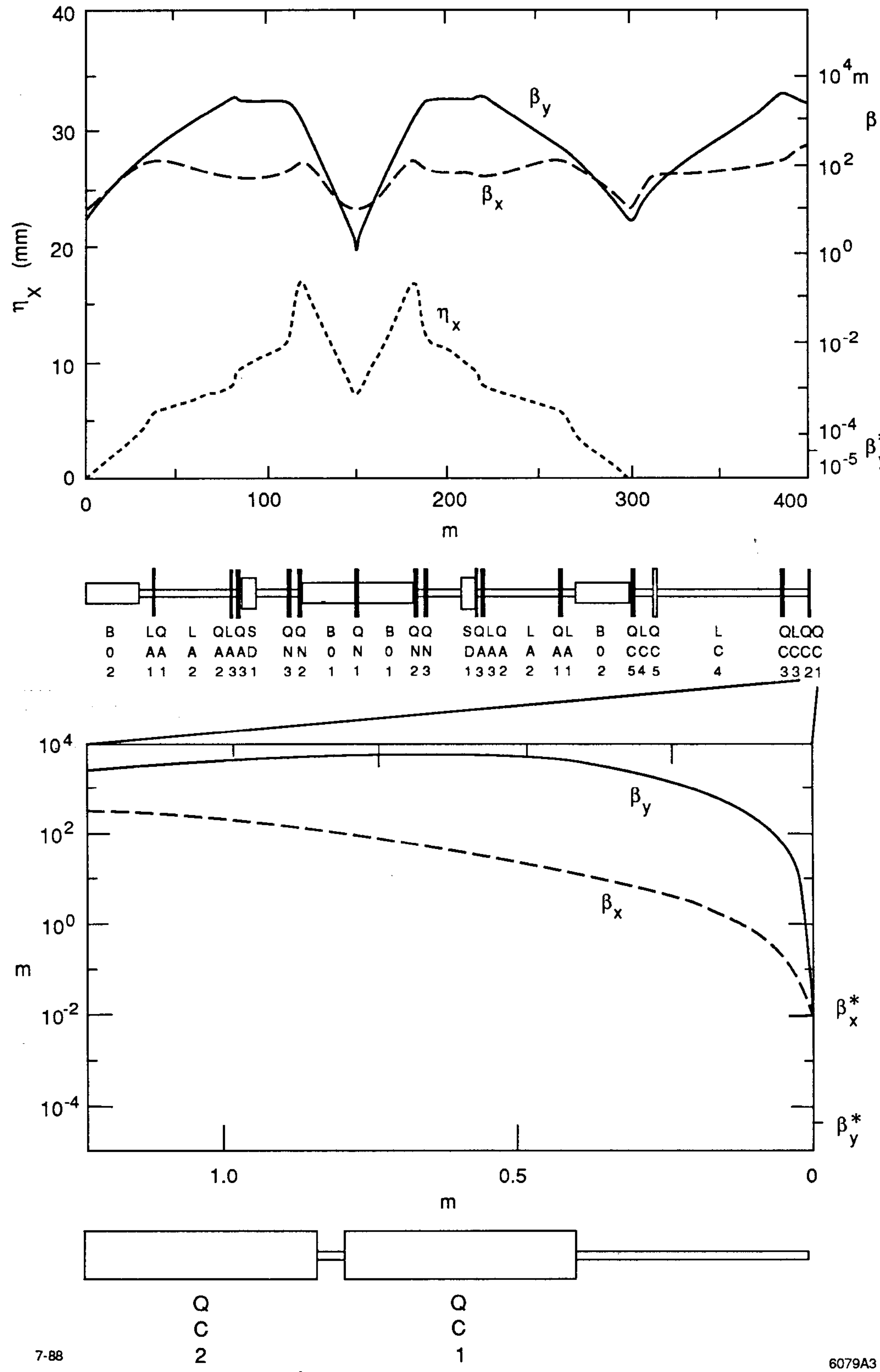

40
30
20
10
0
η_x (mm)
10^4m
β
10^2
10^0
10^{-2}
10^{-4}
10^{-5} β_y^*
β_y
β_x
η_x
0
100
200
300
400
m
B 0 2
LQ AA 11
L A 2
QLQS AAAD 2331
QQ NN 32
B 0 1
Q N 1
B 0 1
QQ NN 23
SQLQ DAAA 1332
L A 2
QL AA 11
B 0 2
QLQ CCC 545
L C 4
QLQQ CCCC 3321
10^4
10^2
10^0
10^{-2}
10^{-4}
m
β_y
β_x
β_x^*
β_y^*
1.0
0.5
0
m
Q C 2
Q C 1
7-88
6079A3

Fig. 3

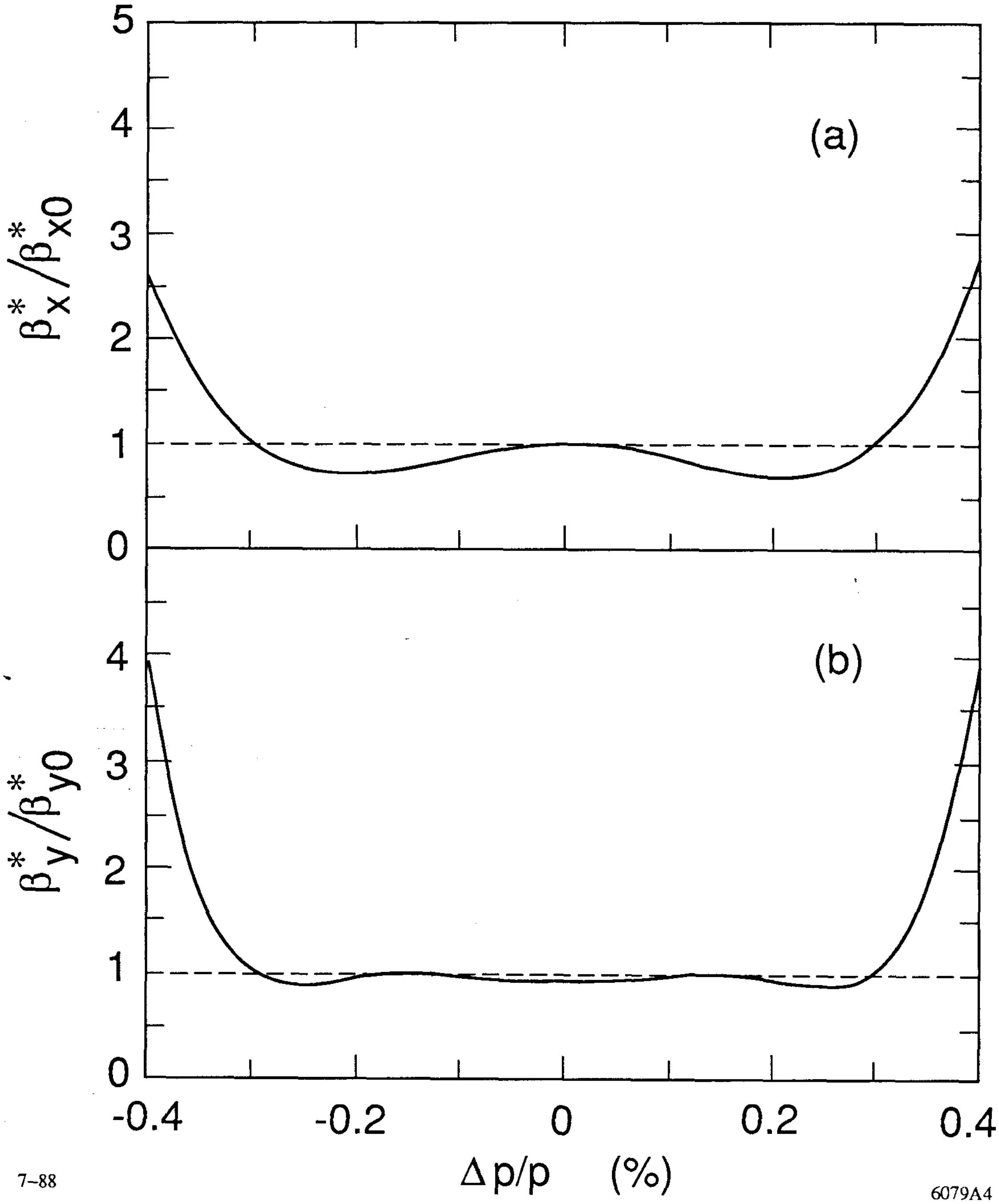

5
4
3
2
1
0
(a)
β_x^*/β_{x0}^*
4
3
2
1
0
(b)
β_y^*/β_{y0}^*
-0.4
-0.2
0
0.2
0.4
$\Delta p/p$ (%)
7–88
6079A4

Fig. 4

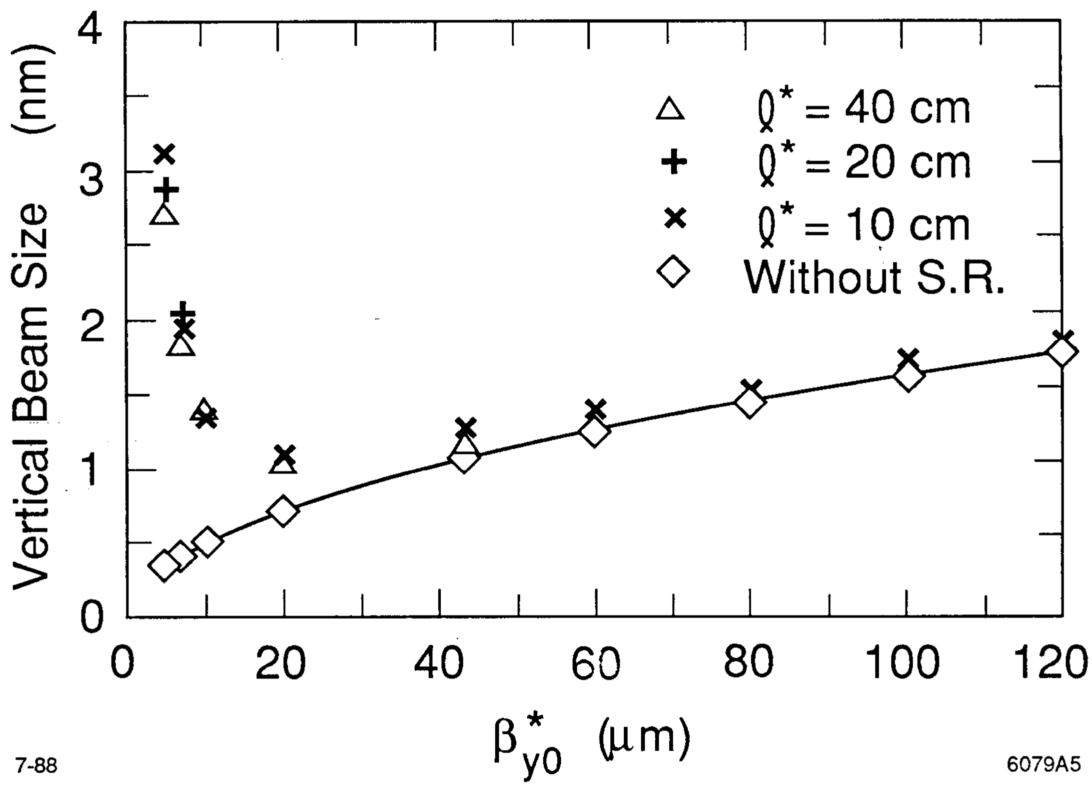

Vertical Beam Size (nm)
0
1
2
3
4
0
20
40
60
80
100
120
$\ell^* = 40$ cm
$\ell^* = 20$ cm
$\ell^* = 10$ cm
Without S.R.
β^*_{y0} (μm)
7-88
6079A5

Fig. 5

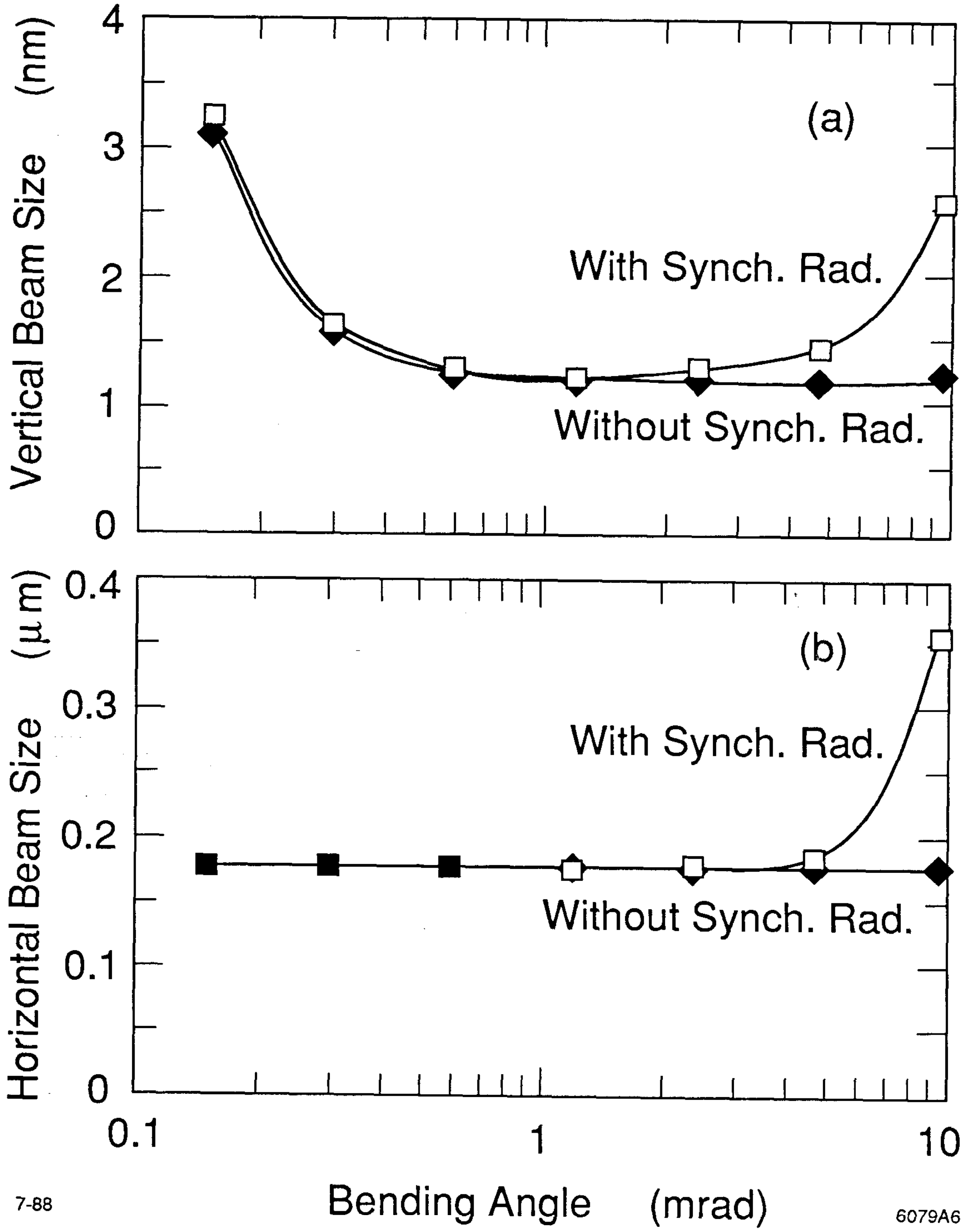

7-88

6079A6

Fig. 6